European Review for Medical and Pharmacological Sciences 2019; 23: 3984-3992

MiR-21 regulates pulmonary hypertension in rats *via* TGF-β1/Smad2 signaling pathway

F. DING, T. YOU, X.-D. HOU, K. YI, X.-G. LIU, P. ZHANG, X.-K. WANG

Department of Cardiovascular, Gansu Province Hospital, Lanzhou, China

Abstract. – OBJECTIVE: To investigate the effects of micro ribonucleic acid (miR)-21 on pulmonary hypertension (PH) in rats *via* regulating tumor growth factor-β1 (TGF-β1)/mothers against decapentaplegic homolog 2 (Smad2) signaling pathway and the possible underlying mechanism.

MATERIALS AND METHODS: MiR-21 inhibition vector (pLKO-anti-miR-21) was first constructed. The rat model of PH was established by hypoxia feeding induction. A total of three groups were established, including: blank control group, model group and miR-21 low-expression group were set up, with 12 rats in each group. The expression level of miR-21 in tissues of rats in each group was detected by quantitative polymerase chain reaction (qPCR). The right ventricle systolic pressure (RVSP) and right ventricular hypertrophy index (RVHI) of rats in each group were measured. The pathological changes in lung tissues of rats were detected using hematoxylin and eosin (H&E) staining. Terminal deoxynucleotidyl transferase dUTP nick end labeling (TUNEL) staining was used to detect the level of apoptosis in lung tissues of rats in each group. Furthermore, Western blotting was adopted to detect the expression levels of TGF-β1/Smad2 signal pathway-related proteins and apoptosis-related proteins in lung tissues of rats in each group.

RESULTS: Compared with the blank control group, the expression level of miR-21 in lung tissues of rats in model group was significantly increased ($p<0.01$). Meanwhile, miR-21 expression in lung tissues of rats in miR-21 low-expression group was significantly decreased by transfection of miR-21 inhibition vector ($p<0.01$). The RVSP and RVHI of rats in model group were significantly higher than those in blank control group and miR-21 low-expression group ($p<0.01$). H&E staining results indicated that the degree of lung tissue injury in model group was remarkably higher than in blank control group and miR-21 low-expression group ($p<0.01$). According to TUNEL staining results, the number of apoptotic cells in lung tissues of rats in model group was markedly smaller than that of miR-21 low-expression group ($p<0.01$). Moreover, the expression level of Caspase 3 in lung tissues of rats in model group was significantly lower than that of miR-21 low-expression group, while the expression level of B-cell lymphoma 2 (Bcl-2)/Bcl-2-associated X protein (Bax) was markedly higher. The expression levels of TGF-β1 and phosphorylated (p)-Smad2 in lung tissues of rats in model group were evidently higher than those of blank control group ($p<0.01$). In addition, lowly expressed miR-21 could effectively reduce the expressions of TGF-β1 and p-Smad2 ($p<0.01$).

CONCLUSIONS: MiR-21 regulates the symptoms of PH in rats by activating TGF-β1/Smad2 signaling pathway.

Key Words

MiR-21, Pulmonary hypertension (PH), TGF-β1/Smad2 signaling pathway.

Introduction

Pulmonary hypertension (PH) is a common cardiovascular disease, which seriously threatens human life and health. Research evidence has shown that the average survival time of PH patients is only 1.9 years after the occurrence of significant clinical symptoms[1]. The main pathological feature of PH is the abnormal increase in pulmonary vascular resistance. This may lead to continuous proliferation of pulmonary arteries and reconstruction of pulmonary vessels, eventually causing right heart failure and even death[2]. At present, the pathogenesis of PH remains unclear. Various factors can lead to increased blood flow and resistance of pulmonary circulation, thus inducing the occurrence of multiple diseases. Therefore, most current treatment methods cannot effectively improve the pathological state of patients with PH. Furthermore, this may lead to poor prognosis of patients[3,4]. Therefore, the key to effective treatment of PH is to find new targets and discoveries through in-depth analysis of the molecular mechanism of PH.

Corresponding Author: Xinkuan Wang, MM; e-mail: 308741084@qq.com

A large number of studies[5,6] have found that micro ribonucleic acids (miRNAs) participate in the physiological and pathological processes of various diseases, such as cell differentiation, proliferation and apoptosis. MiR-21 involves in vascular tension and relaxation, reduces the apoptosis of vascular cells, and participates in vascular remodeling through multiple signaling pathways[7]. At the same time, over-expression of miR-21 inhibits the apoptosis of myocardial cells. Pariskh et al[8] have found that the expression level of miR-21 in myocardial cells of rats with myocardial ischemia is significantly increased. Meanwhile, over-expression of miR-21 can notably reduce the apoptosis of myocardial cells. Research evidence has suggested that the tumor growth factor-β1 (TGF-β1)/mothers against decapentaplegic homolog 2 (Smad2) signaling pathway is involved in the process of pulmonary vascular remodeling. Bai et al[9] have indicated that activation of the TGF-β1/Smad2 signaling pathway promotes fibrosis after myocardial injury, in which TGF-β1 plays a vital role. However, few studies have investigated the regulatory effect of miR-21 on TGF-β1/Smad2 as well as its role in pulmonary hypertension. In this study, a rat model of PH was established by hypoxia feeding induction. Moreover, we evaluated the effect of miR-21 on PH in rats and further explored the regulatory effect of miR-21 on TGF-β1/Smad2 signaling pathway.

Materials and Methods

Construction of the miR-21 Interference Vector

The sequence of mmu-miR-21 was obtained. MiR-21 inhibitor anti-miR-21 was synthesized by Shanghai GenePharm Co., Ltd. (Shanghai, China). SiRNA oligo sequence was 5-UCAACAUCAGUGAGAUCUUCUA-3. After transfection of anti-miR-21 for 48 h, the transfection efficiency was measured. Finally, successfully transfected plasmid was selected to prepare the miR-21 interference vector (pLKO-anti-miR-21).

Animal Grouping And Model Construction

Sprague-Dawley (SD) rats (250-280 g) were purchased from Guangdong Medical Laboratory Animal Center. All rats were raised in Specific-Pathogen-Free (SPF) animal houses with a temperature of (25±1)°C and a humidity of (45±2)%. According to the circadian rhythm, all animals had free access to food and water. After one week's adaptation to the environment, SD rats were randomly divided into blank control group, model group and miR-21 low expression group. 12 rats were included in each group after ensuring the success of model construction. The rat model of PH was established by induction *via* hypoxia feeding. Rats in the control group were raised in normal environment, while those in model group and miR-21 low expression group were raised in hypoxia incubator. Besides, rats in miR-21 group were injected with pLKO-Anti-miR-21 plasmid via pulmonary arteries. This study was approved by the Laboratory Animal Ethics Committee of the hospital. All animal operations were carried out in accordance with the relevant provisions of the NIH Laboratory Animal Guide.

Establishment of the model: rats were fed in a hypoxia incubator (filled gas of 90% nitrogen and 10% oxygen) for 8 h every day in hypoxic environment. After 3 weeks, the success of establishment of the model was evaluated (hypoxia treatment time could be appropriately prolonged to ensure the success of the model establishment).

Measurement of the Right Ventricle Systolic Pressure (RVSP) and Right Ventricular Hypertrophy Index (RVHI) in Rats

The rats were first anesthetized by intraperitoneal injection of 5% chloral hydrate. Then the rats were fixed on the experimental operating table. RVSP of rats in each group was measured using a right cardiac catheter and recorded. After the rats were killed, heart samples were separated, and the right ventricle free wall (RV) and left ventricle + ventricular septum (LV+S) were removed. Finally, the RVHI was calculated after weighing based on the following formula: RVHI=RV/(LV+S).

Pathological Changes in Lung Tissues of Rats

Hematoxylin and eosin (H&E) staining (Boster, Wuhan, China) was used to detect the pathological changes of lung tissues in rats of each group. After killed, lung tissues of rats in each group were separated and rinsed with pre-cooled phosphate-buffered saline (PBS) to remove blood stains. After fixing with paraformaldehyde, the lung tissues were dehydrated with different concentrations of ethanol, followed by transparency with xylene. Then the lung tissues were embedded with paraffin and sliced into 5 μm-thick sections. After dewaxing, the sections were hydrated

with 95%, 90%, 80%, 75% and 50% ethanol, respectively. Subsequently, they were stained with hematoxylin and eosin, respectively. After staining, the sections were dehydrated with different concentrations of ethanol, followed by transparency with xylene and mounting with neutral resin. Finally, the morphological changes in lung tissues of rats in each group were observed under the bright field of microscope.

Detection of Apoptosis via Terminal Deoxynucleotidyl Transferase dUTP Nick End Labeling (TUNEL) Assay

Lung tissue sections of rats in each group were dewaxed into water, treated with prepared 3% hydrogen peroxide for 10 min and washed with PBS for 3 times. After that, proteinase K solution was added to the sections, followed by digestion at 37°C in a wet box for 10 min. Then, the sections were washed with PBS for 3 times. Subsequently, 40 μL mixed solution of TdT and DIG-d-UTP was added. The sections were labeled in a wet box at 4°C for 2 h and washed with PBS for 3 times. Next, the sections were incubated with 40 μL sealing solution at room temperature for 30 min. The antibody was added for incubation in a wet box at 37°C for 40 min, followed by washing with PBS for 3 times. The sections were incubated with strept avidin-biotin complex-fluorescein isothiocyanate (SABC-FITC) secondary antibody (1:100) (Solarbio, China) at 37°C in a wet box for 40 min. Anti-fluorescence quenching sealing liquid was added dropwise for mounting. Finally, the sections were photographed under an inverted fluorescence microscope. Cells with yellow-green fluorescence were TUNEL-positive cells, namely apoptotic cells. TUNEL positive rates were calculated from 10 fields of view.

Real-Time Quantitative Polymerase Chain Reaction (qPCR)

Lung tissues of rats in each group were collected, and added with RIzol reagent (TRIzol kit, ThermoFisher Scientific, Waltham, MA, USA) at the ratio of 100 mg: 1 mL after weighing. After that, lung tissues were homogenized on an icebox until no tissue fragments were visible to naked eyes. After standing for 5 min, 200 μL chloroform was added, followed by centrifugation at 4°C and 12000 rpm for 10 min. Subsequently, the supernatant was taken, and equal volume of isopropyl alcohol was added for centrifugation at 4°C and 12000 rpm for 10 min. The supernatant was discarded, and freshly prepared 75% ethanol was added for centrifugation at 4°C and 2000 rpm for 10 min. Finally, the supernatant was removed and 30 μL diethyl pyrocarbonate (DEPC) (Beyotime, Shanghai, China) was added to dissolve precipitates. The product was total RNA solution. The purity and concentration of RNA were quantified through monitoring. Reverse transcription PCR (RT-PCR) was then conducted to obtain complementary deoxyribonucleic acid (cDNA) strands. Subsequently, they were taken as templates for qPCR in strict accordance with SYBR ExScript™ RT-PCR kit (TaKaRa, Otsu, Shiga, Japan). Reaction conditions were set as follows: 94°C for 4 min, 94°C for 30 s and 72°C for 30 s for a total of 35 cycles, and 72°C for 5 min. Primers were synthesized by Invitrogen (Carlsbad, CA, USA), and sequences were shown in Table I. Glyceraldehyde-3-phosphate dehydrogenase (GAPDH) was used as the internal reference. The relative expression level of miR-21 in lung tissues of rats in each group was calculated by the $2^{-\Delta\Delta Ct}$ method.

Western Blotting

After rats in each group were euthanized, lung tissues were separated and added with radio-immunoprecipitation assay (RIPA) lysate (Beyotime Biotechnology Co., Ltd., Shanghai, China) at a ratio of 100 mg: 1 mL after weighing. After adding 1% protease inhibitor and 1% phosphatase inhibitor, they were homogenized on an ice box by ultrasonic homogenizer. The concentration of extracted total protein in lung tissues of rats in each group was detected by the bicinchoninic acid (BCA) Protein Determination Kit (R&D Systems, Minneapolis, MN, USA). A sample loading

Table I. qPCR primers.

RNA	Sequence
miR-21	Forward primer: 5'-CCGGTCAAGAGAGAGAGAGAGATA-3' Reverse primer: 5'-GGTCTGTACAATCTACGGT-3'
GAPDH	Forward primer: 5'-CAGTGCCAGCCTCGTCTCAT-3' Reverse primer: 5'-AGGGCCATCCACAGTCTTC-3'

system of equal concentration was prepared and boiled at 95°C. Subsequently, the proteins were separated by sodium dodecyl sulphate (SDS) gel at 80 V and transferred onto membranes at 100 V using the wet membrane transfer method. Then, the membranes were blocked with freshly prepared 5% skim milk powder at room temperature for 2 h. Target bands were cut according to the molecular weight of target proteins. The membranes were incubated with primary antibodies of b-cell lymphoma 2 (Bcl-2), Bcl-2-associated X protein (BAX), Bax, Caspase-3, TGF-β1, Smad2, phosphorylated (p)-Smad2 and GAPDH (antibodies were purchased from CST and diluted at 1:1000, Danvers, MA, USA) at 4°C overnight. After washing with Tris-buffered saline and Tween-20 (TBST) for 3 times, the membranes were incubated with secondary antibody conjugated with horseradish peroxidase (HRP) (Shanghai Yihyson Biotechnology Co., Ltd. Shanghai, China) at room temperature for 1 h. After washing with TBST for 3 times, freshly prepared electrochemiluminescence (ECL) mixture was added (Thermo Fisher Scientific, Waltham, MA, USA). The bands were treated with software after color development in dark. Ultimately, the expression level of corresponding proteins in each group was calculated.

Statistical Analysis

Statistical Product and Service Solutions (SPSS) 22.0 software (IBM Corp. Armonk, NY, USA) was used for all statistical analysis. All data were all expressed by ($\bar{x}\pm SE$). One-way ANOVA was used to compare the differences among different groups, followed by Post Hoc Test LSD (Least Significant Difference). After homogeneity of variance test, Bonferroni test was used in the case of homogeneity of variance. Meanwhile, Games-Howell test was adopted in the case of heteroscedasticity of variance. $p<0.05$ was considered statistically significant.

Results

Expression Level of miR-21 in Lung Tissues of Rats

Real-time qPCR was performed to detect the expression level of miR-21 in lung tissues of rats in each group. The results revealed that compared with blank control group, the expression level of miR-21 in lung tissues of rats in model group was significantly increased ($p<0.01$). Meanwhile, miR-21 expression in miR-21 low-expression group was significantly reduced after transfection of the miR-21 inhibition vector ($p<0.01$) (Figure 1).

Detection of the RVSP and RVHI of Rats in Each Group

After anesthesia, the RVSP of rats in each group was measured by a right cardiac catheter. The right ventricle was separated to calculate the RVHI. As shown in Figure 2, the RVSP and RVHI of rats in model group were markedly higher than those of blank control group ($p<0.01$) and miR-21 low-expression group (p

Pathological Changes in Lung Tissues of Rats in Each Group

The pathological changes of lung tissues in rats of each group were detected by H&E staining. Results manifested that compared blank control group, lung tissues of rats in model group were significantly thickened with a large number of infiltration of inflammatory cells and edema, fibrosis and bleeding in alveoli. Moreover, the degree of injury in miR-21 low-expression group was significantly reduced (Figure 3).

Apoptosis Level in Lung Tissues of Rats in Each Group

TUNEL staining was adopted to detect the level of apoptosis in lung tissues of rats in each group. As shown in Figure 4, there were no obvious TUNEL-positive cells in lung tissues of

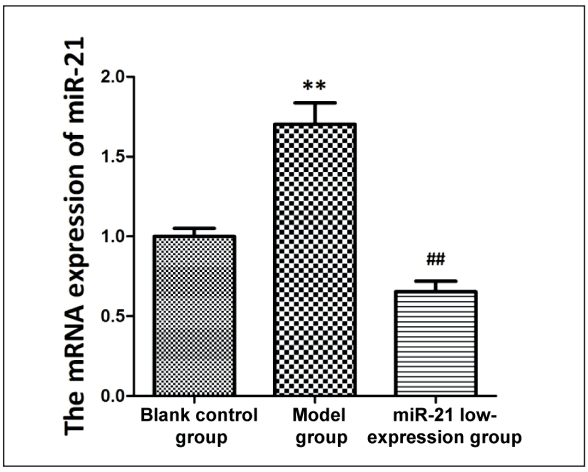

Figure 1. Expression level of miR-21 in lung tissues of rats in each group detected via Real-time qPCR. The expression level of miR-21 in lung tissues of rats in model group was significantly higher than those of blank control group and miR-21 low-expression group. $^{**}p<0.01$ *vs.* blank control group and $^{\#\#}p<0.01$ vs. model group.

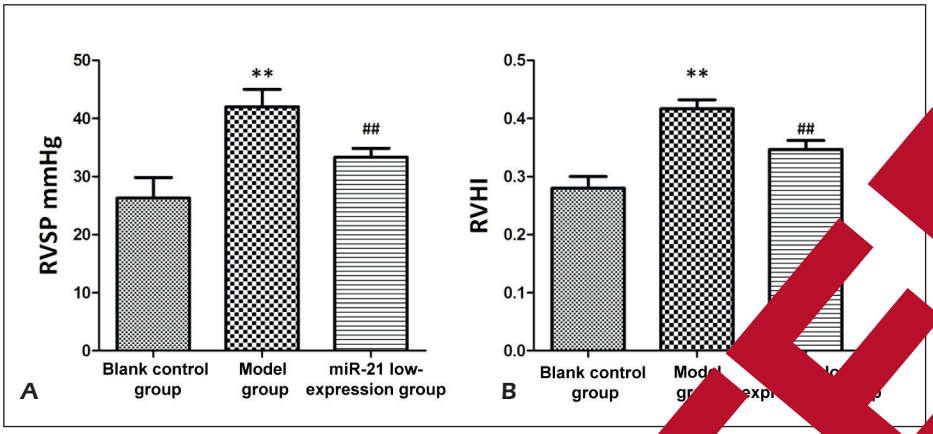

Figure 2. Detection of the RVSP and RVHI of rats. The RVSP and RVHI of rats in [illegible] group were notably higher than those of blank control group and miR-21 low-expression group. **p<0.01 vs. blank control [illegible] p<0.01 *vs.* model [illegible] up.

rats in blank control group and model group. Furthermore, the number of TUNEL-positive cells in lung tissues of rats in miR-21 low-expression group was evidently larger than that of model group (p<0.01).

Expression Level of Apoptotic Proteins in Lung Tissues of Rats in Each Group

The expression level of apoptotic protei[n] lung tissues of rats in each group was detec[ted] *via* Western blotting. Results d[emon]strated th[at] the protein expression level o[f] in lung tissues of rats in model gr[oup] was s[ignif]icantly lower than that of miR-2[1] low-expre[ssion] group (p<0.01). However, the p[rotein] ex[pression] of Bcl-2/Bax was re[markab]ly [higher] than that of miR-21 low-expres[sion] group (p[<0.01] (Figure 5).

Mi[R-21] Regulated TG[F-β1]/Smad2 Signaling Pathway

Western blot[ting] was carried out to detect the [expr]ession level[s] of proteins related to TGF-β1/S[mad2] signalin[g] pathway in lung tissues of rats in e[ach] [group]. Results found that the expression levels of TGF-β1 and p-Smad2 in lung tissues of rats in model group were notably higher than [those] of blank control group (p<0.01). Moreover, [low] expression of miR-21 could effectively reduce the expressions of TGF-β1 and p-Smad2 (p<0.01).

Discussion

PH is a clinical syndrome characterized by pulmonary vascular occlusive disease and increased pulmonary circulation pressure induced

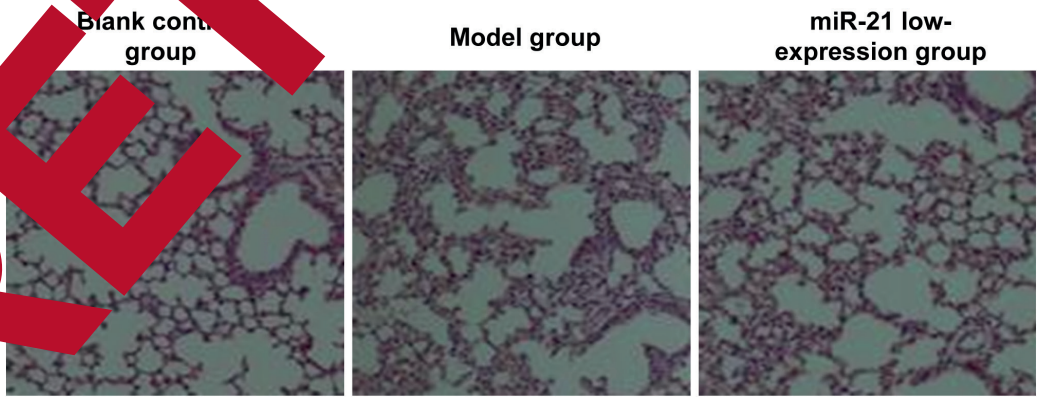

Figure 3. Pathological changes in lung tissues of each group of rats detected via H&E staining (magnification: 100x). In model group, there was a large amount of inflammatory infiltration in lung tissues, edema and fusion appear in the alveoli. The degree of lung tissue injury in miR-21 low-expression group was obviously reduced.

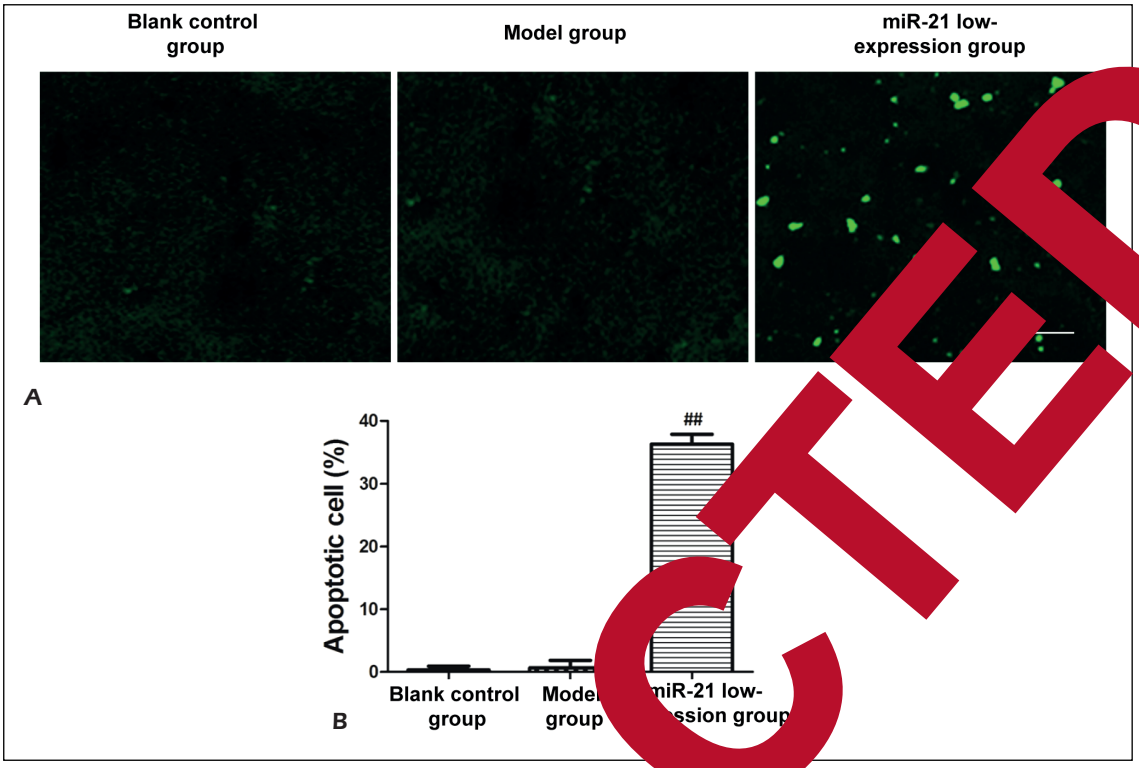

Figure 4. Apoptosis level in lung tissues of rats i…oup detected using TUNEL staining. There were no significant TUNEL-positive cells in lung tissues of rats in blank… model group. The number of TUNEL-positive cells in lung tissues of rats in miR-21 low-expression group was evi… larger… odel group (Bar=50 μm). $^{\#\#}p<0.01$ *vs.* model group.

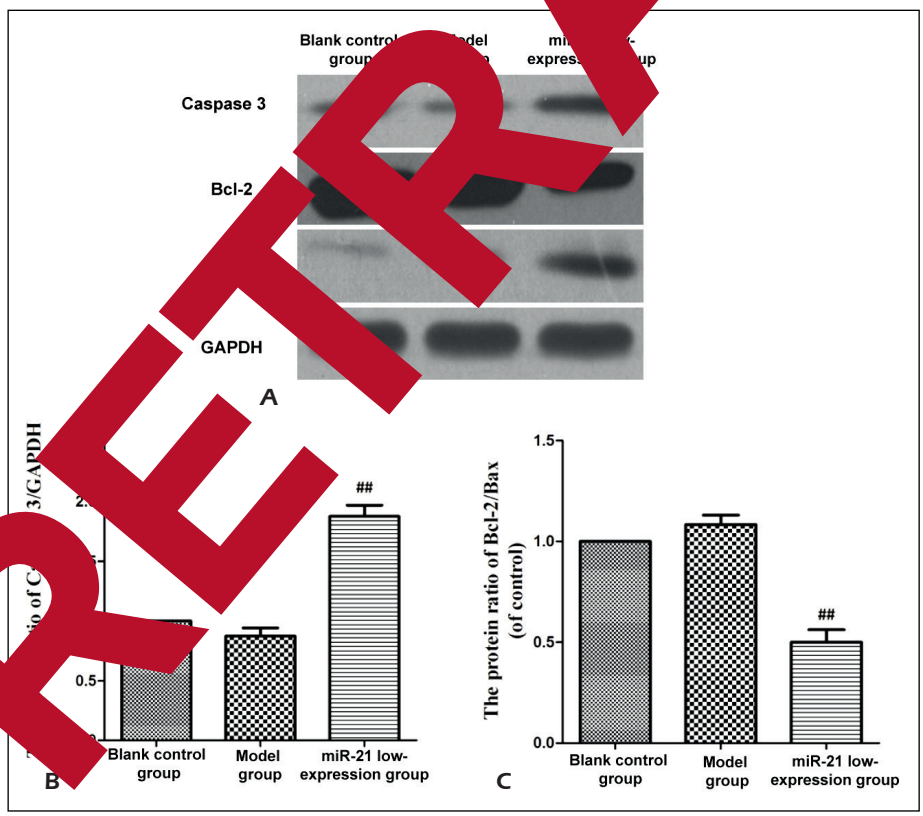

Figure 5. Expression level of apoptotic proteins in lung tissues of rats in each group detected by Western blotting. Compared with model group, the expression level of Caspase 3 in lung tissues of rats in miR-21 low-expression group was evidently increased, while the expression level of Bcl-2/Bax was significantly decreased. $^{\#\#}p<0.01$ *vs.* model group.

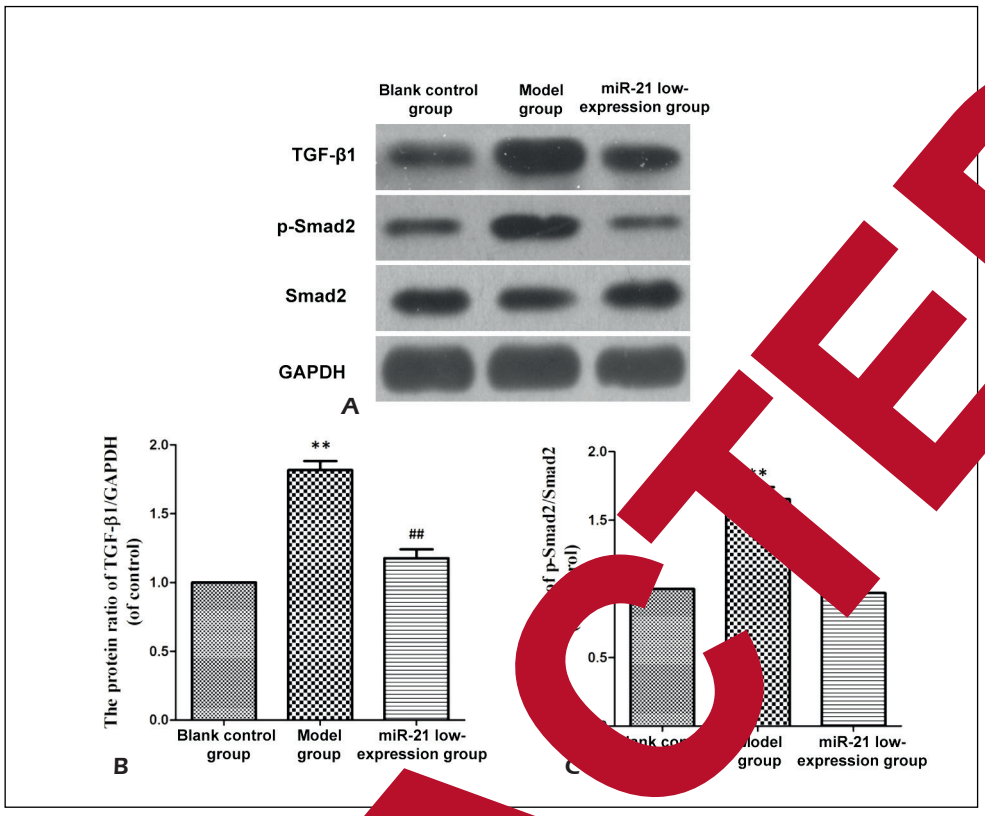

Figure 6. Expression level of proteins related to TGF[illegible]way in lung tissues of rats in each group detected via Western blotting. Compared with blank control group, t[illegible]pressi[illegible]F-β1 and p-Smad2 in lung tissues of rats in model group were significantly increased. Meanwhile, the expre[illegible]le[illegible]l TGF-β1 and p-Smad2 in miR-21 low-expression group were markedly lower than those of model group. $^{**}p<0.01$ *vs.* bl[illegible]ol group and $^{\#\#}p<0.01$ *vs.* model group.

by various factors[10]. In m[illegible]PH p[illegible]nts, the apoptotic level of pulmo[illegible]vascu[illegible]-the-lial cells declines, and th[illegible]life[illegible] increases. This may [illegible]t in [illegible]n of pulmonary blood vessel[illegible]verload o[illegible]ight heart, and even failur[illegible] right heart[illegible]Hypoxia feeding can e[illegible]ve[illegible]ulate the pathogenesis of PH in hu[illegible] body, s[illegible]o stably establish a PH rat m[illegible] It is an impo[illegible]method to study the path[illegible]nesis of PH and to f[illegible] novel treatment plans[illegible]n this[illegible]y, Sprague-Dawley (SD) rats we[illegible]d in h[illegible]xia env[illegible]onment for 21 consecutive[illegible]er the [illegible]el was established, the RVSP an[illegible]II of[illegible]n model group fed in the [illegible]a env[illegible]were significantly increased whe[illegible]ompared[illegible]h those of normal rats. This ind[illegible]d that the model was successfully estab-li[illegible]me time, the results of H&E staining also demonstrated that lung tissues in model [illegible]p were much more seriously injured. Sisniega[illegible][14] found that PH can also lead to secondary l[illegible]g function decline and lung tissue injury. A large amount of research evidence has shown that miR-21 exerts a regulatory effect on many kinds of cells, such as myocardial cells, vascular smooth muscle cells and vascular endothelial cells. Tong et al[15] showed that over-expression of miR-21 was closely related to the proliferation of myocardial cells and myocardial remodeling. In this study, the expression level of miR-21 in lung tissues of rats in each group was further detected through qPCR. The results manifested that the expression level of miR-21 in lung tissues of rats in model group was markedly higher than that of blank control group. Next, RNA interference was used to reduce the expression level of miR-21 in lung tissue of rats in model group. Subsequent results indicated that the RVSP and RVHI of rats in miR-21 low-expression group were significantly reduced. Meanwhile, lung tissue injury was also evidently reduced. These results highly suggest that miR-21 is involved in the regulation of PH which is an important factor affecting PH.

Shi et al[16] have found that increased expression level of miR-21 in myocardial cells of rats significantly reduces the level of apoptosis. In this study,

TUNEL staining was conducted to detect the level of apoptosis in lung tissues of PH model rats. It was observed that the level of apoptosis in lung tissues of rats in miR-21 low-expression group was notably higher than those of model group and blank control group. In addition, Western blotting also demonstrated that the expression levels of apoptosis-related proteins, Caspase 3 and Bcl-2/Bax in lung tissues of miR-21 low-expression group were significantly reduced. Xu et al[17] have also demonstrated that miR-21 plays an anti-apoptotic role by mediating toll-like receptor (TLR) signaling pathway, regulating TLR4 and inhibiting the expression of programmed death factor 4. This can eventually activate NF-κB. Moreover, Iliopoulos et al[18] have also indicated that miR-21 plays an anti-apoptotic role by mediating immune and inflammatory responses.

TGF-β1, as a multifunctional cell activity regulator, plays a regulatory role in the differentiation, proliferation and apoptosis of smooth muscle cells and vascular fibroblasts. After TGF-β1 is activated and binds to the receptor, it can further activate the phosphorylation of its downstream protein Smad2. Meanwhile, p-SMAD3 can bind to regulatory SMAD protein and transfer to the nucleus, thereby playing a vital role[19]. Liao et al[20] identified that the activation of TGF-β1/Smad2 signaling pathway promotes the proliferation and migration of smooth muscle cells. This leads to increased vascular resistance and induces vascular remodeling. It was found in this study that the expression levels of TGF-β1 and p-Smad2 in lung tissues of rats in model group were significantly increased. Suppressing the expression of miR-21 in lung tissues could alleviate the symptoms of PH in rats, which could effectively reduce the expressions of TGF-β1 and p-Smad2 in lung tissues as well. These results indicate that activation of the TGF-β1/Smad2 signaling pathway may be an important cause of PH occurrence. Furthermore, miR-21 may play a regulatory role in PH in rats by activating TGF-β1/Smad2 signaling pathway.

Conclusions

In conclusion, that miR-21 regulates the symptoms of PH in rats by activating TGF-β1/Smad2 signaling pathway. MiR-21 can be used as an indicator for the efficacy of patients with PH, which can also be applied to evaluate the efficacy and prognosis of patients.

Conflict of Interests

The authors declare no conflict of interest.

References

1) Aguirre MA, Lynch I, Ha[illegible]n B. [illegible]rative management of pulm[illegible]y hyperten[illegible] right ventricular failur[illegible]ng non-cardiac s[illegible] Adv Anesth 2018; [illegible]01-230.
2) Latham GJ, Yung[illegible]urrent [illegible]erstand[illegible]g and perioperative [illegible] [illegible] pediatr[illegible]ulmonary hyperte[illegible]n. F[illegible] Anaes[illegible]018; 8: 73-80.
3) Klok FA, [illegible]S, Konstantin[illegible] [illegible]artevelle P, Fadel [illegible] [illegible] Kim NH, Ma[illegible]M, Matsubara H, M[illegible]E, Pe[illegible] J, Delcroix M, Lang IM. Determinants of dia[illegible]e delay in chronic thromb[illegible]olic pulmona[illegible]rtension: results from [illegible]opean CTEPH r[illegible]try. Eur Respir J 2018; [illegible]. 48-63.
4) Araszkiewicz A, [illegible]arocha S, Pietrasik A, Pietura R, Jankiewicz S, [illegible]szkiewicz M, Slawek-Szmyt S, Bie[illegible]erman A, M[illegible]ek-Kubzdela T, Lesiak M, Torbicki [illegible]Kurzyna M[illegible]lloon pulmonary angioplasty for [illegible]f residual or recurrent pulmonary hy[illegible]n after pulmonary endarterectomy. Int J Cardiol 2018; 8: 15-26.
5) Zhu G, Zhang W, Liu Y, Wang S. miR371b5p inhibits [illegible]helial cell apoptosis in monocrotaline in[illegible]d pulmonary arterial hypertension via PTEN/PI3K/Akt signaling pathways. Mol Med Rep 2018; 18: 5489-5501.
6) Liang Z, Chi YJ, Lin GQ, Luo SH, Jiang QY, Chen YK. MiRNA-26a promotes angiogenesis in a rat model of cerebral infarction via PI3K/AKT and MAPK/ERK pathway. Eur Rev Med Pharmacol Sci 2018; 22: 3485-3492.
7) Iannone L, Zhao L, Dubois O, Duluc L, Rhodes CJ, Wharton J, Wilkins MR, Leiper J, Wojciak-Stothard B. miR-21/DDAH1 pathway regulates pulmonary vascular responses to hypoxia. Biochem J 2014; 462: 103-112.
8) Parikh VN, Jin RC, Rabello S, Gulbahce N, White K, Hale A, Cottrill KA, Shaik RS, Waxman AB, Zhang YY, Maron BA, Hartner JC, Fujiwara Y, Orkin SH, Haley KJ, Barabasi AL, Loscalzo J, Chan SY. MicroRNA-21 integrates pathogenic signaling to control pulmonary hypertension: results of a network bioinformatics approach. Circulation 2012; 125: 1520-1532.
9) Bai YW, Ye MJ, Yang DL, Yu MP, Zhou CF, Shen T. Hydrogen sulfide attenuates paraquat-induced epithelial-mesenchymal transition of human alveolar epithelial cells through regulating transforming growth factor-beta1/Smad2/3 signaling pathway. J Appl Toxicol 2018; 3: 61-75.
10) Ng QX, Venkatanarayanan N, Ho C, Sim WS, Lim DY, Yeo WS. Selective serotonin reuptake inhibitors and persistent pulmonary hypertension of the newborn: an update meta-analysis. J Womens Health (Larchmt) 2018; 7: 195-207.

11) Li D, Sun Y, Kong X, Luan C, Yu Y, Chen F, Chen P. Association between a single nucleotide polymorphism in the 3'-UTR of ARHGEF18 and the risk of nonidiopathic pulmonary arterial hypertension in chinese population. Dis Markers 2018; 2018: 2461845.
12) Yoon KL. New therapeutic target for pulmonary arterial hypertension. Korean Circ J 2018; 48: 1145-1147.
13) Lee DS, Jung YW. Protective effect of right ventricular mitochondrial damage by cyclosporine A in monocrotaline-induced pulmonary hypertension. Korean Circ J 2018; 48: 1135-1144.
14) Sisniega C, Zayas N, Pulido T. Advances in medical therapy for pulmonary artery hypertension. Curr Opin Cardiol 2018; 5: 116-127.
15) Tong Z, Tang Y, Jiang B, Wu Y, Liu Y, Li Y, Xiao X. Phosphorylation of nucleolin is indispensable to upregulate miR-21 and inhibit apoptosis in cardiomyocytes. J Cell Physiol 2018; 5: 116-127.
16) Shi B, Wang Y, Zhao R, Long X, Deng W, Wang Z. Bone marrow mesenchymal stem cell-derived exosomal miR-21 protects C-kit+ cardiac stem cells from oxidative injury through the PTEN/PI3K/Akt axis. PLoS One 2018; 13: e191616.
17) Xu R, Huang H, Han Z, Li M, Zhou X. [illegible] of TLR-4/MyD88 signaling cascade [illegible] is involved in airway immunological dysfunction induced by cold air exposure[illegible] Fang Yi Ke Da Xue Xue Bao 2016; 36: 98-[illegible]
18) Iliopoulos D, Kavousanaki M, Ioannou [illegible] Vaxevanis D, Verginis P. The negative co[illegible]latory m[illegible]PD-1 modulates the balance [illegible]en immunity a[illegible] ance via miR-21. Eur [illegible]munol 20[illegible]41: 1754
19) Lin L, Li R, Cai M[illegible]ang J[illegible]ng W, Guo Y, Yang L, Yang G[illegible] Zh[illegible]Androg[illegible]holide ameliorates li[illegible]fib[illegible]ce: inv[illegible]ent of TLR4/NF-ka[illegible] and [illegible]ta1/S[illegible] signaling pathw[illegible]Oxid Med C[illegible]018; 2018: 780865[illegible]
20) Liao K[illegible]ia K. SB4315[illegible] inhibited cigarette [illegible]oke ext[illegible]duced invasiveness of A549 cells via the TGF[illegible]/Smad2/MMP3 pathway. [illegible]ett 2018; 15: [illegible]686.